

Characterization of Superoxide-Metalloporphyrin Reaction Products: Effective Use of Deuterium NMR Spectroscopy

Ataollah Shirazi and Harold M. Goff*

Contribution from the Department of Chemistry, University of Iowa, Iowa City, Iowa 52242.
Received March 29, 1982

Abstract: Nuclear magnetic resonance spectroscopy has been utilized to define the solution electronic structures of complexes generated from combination of superoxide ion with iron(II) and manganese(II) porphyrins. Very large proton NMR line widths for the iron porphyrin product dictated the use of deuterium NMR for selectively deuterated synthetic porphyrins. On the basis of the pyrrole deuterium signal at 60 ppm (Me_2SO solvent, 28 °C, Me_4Si reference) and a solution magnetic moment of $\geq 5.6 \mu_B$, a peroxoiron(III) porphyrin structure consistent with an earlier formulation is favored. A corresponding manganese porphyrin signal at 32 ppm and a solution magnetic moment of $5.0 \mu_B$ are indicative of a superoxomanganese(II) porphyrin configuration with spin coupling between the superoxide ligand and the manganese center. This species provides an excellent model for what has been described as superoxide coupling to a low-spin iron(III) center in the oxyhemoglobin molecule. The peroxoiron porphyrin complex is likely coordinated in the second axial position by a solvent molecule. The axial ligand combination leaves the iron center in a high-spin state, but the peroxo ligand serves to reduce the zero-field-splitting value and indirectly induce large NMR line widths. Variable-temperature NMR Curie law behavior is consistent with monomeric structures. Absence of splitting in the pyrrole signals suggests no attack of porphyrin nitrogen atoms by peroxide or superoxide species.

Introduction

The biological action of dioxygen and its reduced states (O_2^- , O_2^{2-}) is largely directed by metalloenzymes. In this regard, the extensive redox and coordination chemistry of the iron porphyrin prosthetic group (along with perturbations of amino acid binding) make possible the oxygen transport, oxygen activation, respiration, and peroxide destruction functions of hemoproteins. Simple metalloporphyrins have provided a wealth of information concerning reversible dioxygen coordination,¹ but the reactive oxygen adducts of other iron porphyrin intermediates have not received corresponding attention. Superoxide ion is not a usual substrate for hemoproteins but formally is an important resonance configuration for oxygenated hemoglobin and cytochrome P-450. Valentine and co-workers have examined various reactions of superoxide ion with metalloporphyrins.²⁻⁵ Among complexes studied in detail, one of the most novel is formed by coordination of iron(II) tetraphenylporphyrin with O_2^- in aprotic solvents such as dimethyl sulfoxide (Me_2SO) or acetonitrile.⁵ On the basis of ESR and vibrational spectral measurements the complex has been formulated as a bidentate peroxoiron(III) porphyrin adduct, $(\text{TPP})\text{FeO}_2^-$.⁵ (Earlier workers described this species as a superoxoiron(II) complex because the visible-UV spectrum does not resemble that of a high-spin iron(III) porphyrin.⁶) Dioxygen binding to the iron(I) tetraphenylporphyrin species reportedly produces an identical complex, for which the solid-state Mössbauer isomer shift value of 0.57 mm/s would suggest a high-spin iron(III) configuration.⁷ The iron octaethylporphyrin derivative, $(\text{OEP})\text{FeO}_2^-$, likewise has been generated by one-electron elec-

trochemical reduction of the dioxygen complex.⁸ Rationale for comprehensive examination of the putative peroxoiron(III) adducts is found in their being isoelectronic with the poorly identified, highly reactive, reduced dioxygen state of cytochrome P-450.

Definitive solution electronic and molecular structural assignments are possible for iron and manganese porphyrin-superoxide reaction products through examination of NMR spectra. Proton NMR spectra of paramagnetic metalloporphyrins frequently prove diagnostic for elucidating spin and oxidation states, in that the direction of contact shifts for certain resonances is associated with unpaired spin in particular d orbitals.⁹ In general, a large downfield shift for the pyrrole proton signals of a metal-TPP complex indicates partial occupation of the σ -type $d_{x^2-y^2}$ orbital, whereas an upfield shift for this signal signifies depopulation of $d_{x^2-y^2}$ and unpaired spin in the π -symmetry d_{xz} , d_{yz} set. Additional information may be gained from signal line widths and the pattern of phenyl resonances for the TPP complex. These correlations are employed for characterization of solution species generated from reactions between superoxide ion and iron(II) or manganese(II) porphyrins.

Experimental Section

Tetraphenylporphyrin derivatives were prepared by standard benzaldehyde-pyrrrole condensation in a propionic acid reflux.¹⁰ Selectively deuterated benzaldehydes were obtained from a commercial source (Merck). Fully deuterated benzaldehyde was prepared from toluene- d_8 via ceric ammonium nitrate oxidation.¹¹ The appropriate phenyl deuterated TPP species was prepared from these benzaldehydes with use of normal (nondeuterated) propionic acid. The TPP-pyrrole- d_8 species was prepared in a simple "one-pot" reaction in which pyrrole proton exchange was effected prior to condensation. To 250 mL of propionic acid anhydride (Aldrich, 97% pure) was added an equivalent amount of D_2O (34.2 mL), and the mixture was brought to reflux for 30 min under a nitrogen blanket. To this propionic acid- d_1 was added 4.6 mL of pyrrole, and a 1-h reflux was carried out under a nitrogen atmosphere. Air was introduced and 6.6 mL of benzaldehyde was added. Reflux was continued

(1) (a) Basolo, F.; Hoffman, B. M.; Ibers, J. A. *Acc. Chem. Res.* **1975**, *8*, 384-392. (b) Collman, J. P. *Ibid.* **1977**, *10*, 265-272. (c) Traylor, T. G. *Ibid.* **1981**, *14*, 102-109. (d) Reed, C. A. *Met. Ions Biol. Syst.* **1978**, *7*, 277-310.

(2) Valentine, J. S.; Curtis, A. B. *J. Am. Chem. Soc.* **1975**, *97*, 224-226.

(3) Valentine, J. S.; Quinn, A. E. *Inorg. Chem.* **1976**, *15*, 1997-1999.

(4) Valentine, J. S. In "Biochemical and Clinical Aspects of Oxygen"; Caughey, W. S., Ed.; Academic Press: New York, 1979; pp 659-677.

(5) McCandlish, E.; Miksztal, A. R.; Nappa, M.; Sprenger, A. Q.; Valentine, J. S.; Stong, J. D.; Spiro, T. G. *J. Am. Chem. Soc.* **1980**, *102*, 4268-4271.

(6) (a) Afanas'ev, I. B.; Prigoda, S. V.; Khenkin, A. M.; Shteinman, A. S. *Dokl. Akad. Nauk SSSR* **1977**, *236*, 641-644. (b) Kol'tover, V. K.; Koifman, O. I.; Khenkin, A. M.; Shteinman, A. S. *Izv. Akad. Nauk SSSR, Ser. Khim.* **1978**, 1690-1691.

(7) Reed, C. A. In "Electrochemical and Spectrochemical Studies of Biological Redox Components"; Kadish, K. M., Ed.; American Chemical Society: Washington, D.C., 1982; *Adv. Chem. Ser. No. 201*, pp 333-356.

(8) Welborn, C. H.; Dolphin, D.; James, B. R. *J. Am. Chem. Soc.* **1981**, *103*, 2869-2871.

(9) (a) Goff, H.; La Mar, G. N.; Reed, C. A. *J. Am. Chem. Soc.* **1977**, *99*, 3641-3646. (b) La Mar, G. N.; Walker, F. A. In "The Porphyrins"; Dolphin, D., Ed.; Academic Press: New York, 1978; Vol. IV, pp 61-157.

(10) Adler, A. D.; Longo, F. R.; Finarelli, J. D.; Goldmacher, J.; Assour, J.; Korsakoff, L. *J. Org. Chem.* **1967**, *32*, 476.

(11) Fajer, J.; Borg, D. C.; Forman, A.; Felton, R. H.; Vegh, L.; Dolphin, D. *Ann. N.Y. Acad. Sci.* **1973**, *206*, 349-364.

for 30 min as prescribed for the usual TPP synthesis.¹⁰ This procedure yields approximately 90 atom % TPP-pyrrole-*d*₈. Purification of metalloporphyrins by silica gel column chromatography followed metal ion insertion by the standard DMF method.¹² Final products were characterized by proton and deuterium NMR spectra,^{9b} visible-UV spectra, and thin-layer chromatography.

All samples were prepared in a Vacuum Atmospheres drybox under a nitrogen atmosphere. Dimethyl sulfoxide was dried and degassed by vacuum distillation from calcium hydride. The solvent was stored over 4-Å molecular sieves in the drybox. Acetonitrile was degassed by freeze-pump-thaw cycles and stored over 3-Å molecular sieves. Iron(III) and manganese(III) porphyrin chloride complexes were weighed into NMR tubes, which were transferred to the drybox. Potassium superoxide (Alfa) was added as the solid (excess) or titrated into the sample with freshly prepared 0.15 M KO₂, 0.08 M dicyclohexyl-18-crown-6 prepared in Me₂SO solvent. Metalloporphyrin concentrations ranged from 1 to 8 mM. Samples for NMR work were kept at 0 °C or were frozen in dry ice if spectral examination was not possible within a few minutes of preparation. Proton spectra at 90 MHz and deuterium spectra at 13.7 MHz were recorded with a JEOL FX-90Q spectrometer. Unless noted otherwise, chemical shift values are referenced to Me₄Si, with downfield shifts being given a positive sign. Magnetic susceptibility measurements were made by the Evans method¹³ for solutions 8 mM in metalloporphyrin containing no excess KO₂. Visible-UV spectra were examined before and after NMR spectroscopic measurements to verify that the predominant solution species were those previously reported.^{3,5}

Results

Iron Porphyrins. Addition of KO₂ to (TPP)FeCl in Me₂SO-*d*₆ was initially monitored by proton NMR spectroscopy. Addition of 1 equiv of KO₂ resulted in reduction of the iron(III) porphyrin to the iron(II) species, as indicated by the appearance of the pyrrole proton signal at ~12 ppm.¹⁴ Addition of a second equivalent of KO₂ caused the disappearance of the 12-ppm peak, and only the broad, overlapping TPP phenyl signals centered at 7.3 ppm with a shoulder at 9.0 ppm were apparent. Problems with sample instability, limited solubility, and dynamic range demands due to the presence of large solvent and crown ether signals precluded reliable detection of very broad signals or those which might occur in the diamagnetic region of the spectrum. These problems were solved, and at the same time unequivocal signal assignments were made through use of deuterium NMR spectroscopy. Accordingly it is appropriate to discuss briefly the application of deuterium NMR to paramagnetic metalloporphyrin compounds.

In a paramagnetic environment deuterium NMR signals are expected to be considerably sharper than those of the proton. For the limit of total dipolar nuclear relaxation by a paramagnetic center, the line width is a function of the square of the gyromagnetic ratio.¹⁵ Thus, the proton line width in hertz could be 42 times that of a corresponding deuterium signal. Although this limiting factor is not realized for the pyrrole proton (280 Hz) and pyrrole deuterium (28 Hz) signals of (TPP)Fe shown in Figure 1, the gain in signal sharpness (in hertz) is nonetheless impressive. The otherwise very broad ortho phenyl proton signal is clearly observable in the deuterium NMR spectrum (this signal overlaps with the para phenyl resonance and the natural-abundance chloroform deuterium signal). Deuterium NMR spectroscopy is seemingly not advantageous for relatively sharp signals, as it would appear that the para phenyl signal is broader in Figure 1c. Likewise, splitting of the meta phenyl deuterium signal is largely lost, as the longer time scale (lower frequency) of deuterium NMR means that phenyl group rotation can average otherwise non-equivalent phenyl signals. As expected, proton and deuterium chemical shift values are equivalent, thus indicating that spin delocalization mechanisms are the same for these two nuclei.

With the potential utility of deuterium NMR spectroscopy having been demonstrated, the technique was applied to the

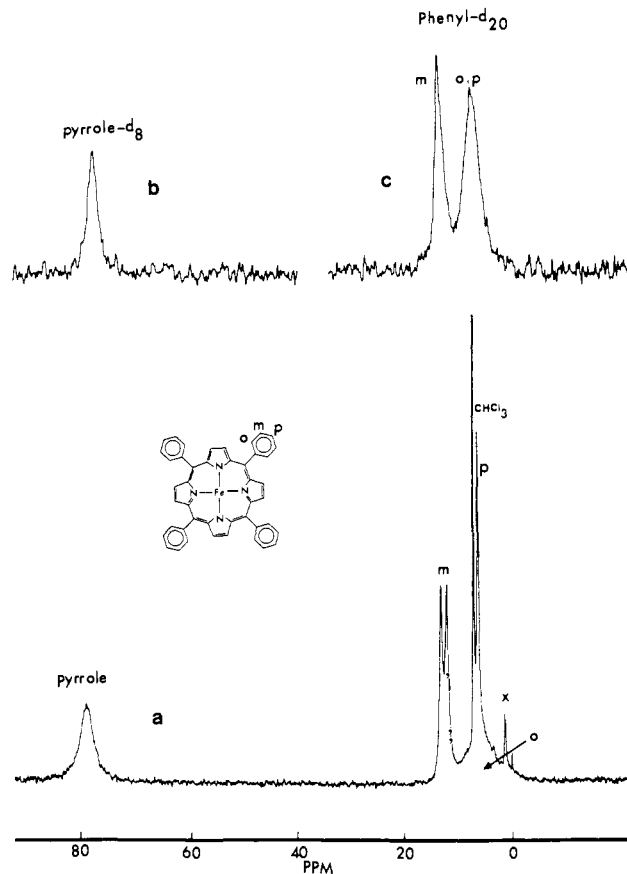


Figure 1. (a) Proton NMR spectrum of (TPP)FeCl, 0.01 M in CDCl₃, at 28 °C, (b) deuterium NMR spectrum of (TPP-pyrrole-*d*₈) FeCl, 0.01 M in CHCl₃, at 28 °C, and (c) deuterium NMR spectrum of (TPP-phenyl-*d*₂₀) FeCl, 0.01 M in CHCl₃, at 28 °C.

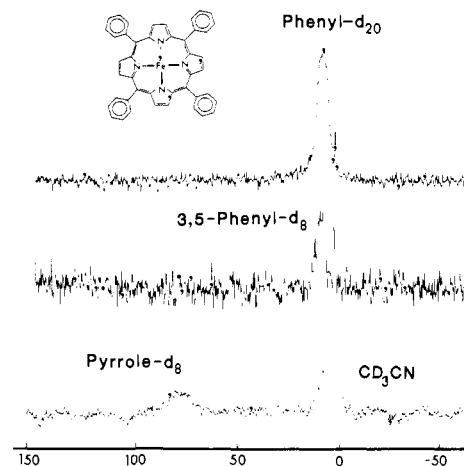


Figure 2. Deuterium NMR spectra of selectively deuterium-labeled (TPP)FeO₂⁻ species, with 6 mM iron porphyrin and CH₃CN solvent at -30 °C. In the bottom spectrum an intense signal is observed for added CD₃CN. The ppm scale is referenced to Me₄Si, and downfield shifts are given positive signs.

deuterated iron porphyrin-superoxide reaction products discussed previously. Figure 2 depicts the 13.7-MHz deuterium NMR spectra of selectively labeled (TPP)Fe in the presence of excess KO₂-crown ether. Acetonitrile was employed as a solvent in this instance to permit low-temperature stabilization of the complex, as well as to conduct variable-temperature NMR measurements. Isotropic shift values were calculated by comparing these observed resonances with those of diamagnetic nickel(II) porphyrin complexes.^{9b} A plot of isotropic shift values vs. 1/T revealed approximate Curie law behavior (the intercept value was -5 ppm for the pyrrole deuterium signal). This demonstrates that the iron porphyrin-superoxide adduct exhibits no large deviation in

(12) Adler, A. D.; Longo, F. R.; Varadi, V. *Inorg. Synth.* **1976**, *16*, 213-220.

(13) Evans, D. F. *J. Chem. Soc.* **1959**, 2003-2005.

(14) Parmely, R. C.; Goff, H. M. *J. Inorg. Biochem.* **1980**, *12*, 269-280.

(15) Swift, T. J. In "NMR of Paramagnetic Molecules"; La Mar, G. N., Horrocks, W. D., Holm, R. H., Eds.; Academic Press: New York, 1973; pp 53-83.

Table I. Proton and Deuterium NMR Data for Various Metalloporphyrin Species^a

spin and oxidn states	species	solvent	temp, °C	nucleus	ref	δ_{pyrrole} , ppm (line width, Hz)	δ_{phenyl} , ppm		
							ortho	meta	para
HS Fe(III)	(TPP)FeO ₂ ⁻	Me ₂ SO	28	² H	<i>b</i>	60 (180)	~7	9.2	7.2
	(TPP)FeO ₂ ⁻	CH ₃ CN	30	² H	<i>b</i>	61 (37)	~7	9.2	7.2
	(TPP)FeCl	CHCl ₃	29	² H	<i>b</i>	78.4 (28)	~6.5	12.7	~6.5
HS Fe(III)	(TPP)FeCl	CDCl ₃	29	¹ H	25b	79.0 (280)	~7	{13.2 12.1	6.35
HS Fe(III)	(TPP)Fe(NO ₃)	CDCl ₃	26	¹ H	24	72.5 (204)	~7	{13.7 12.6	6.4
HS Fe(III)	[(TPP)Fe] ₂ (SO ₄)	CDCl ₃	26	¹ H	24	72.9 (74)	~7	{12.9 11.2	6.4
HS Fe(III)	(TPP)Fe(Me ₂ SO) ₂ ⁺	Me ₂ SO- <i>d</i> ₆	28	¹ H	<i>b</i> , 22a	66.8 (250)		phenyls 12.7, 9.65	
HS Fe(III) dimer	[(TPP)Fe] ₂ O	CDCl ₃	29	¹ H	25a	13.5 (50)		phenyls 7.6	
HS Fe(III) dimer	[(TPP)Fe] ₂ O ₂	toluene- <i>d</i> ₈	-80	¹ H	20	16.0 (80)		phenyls 7.7, 7.6	
<i>S</i> = 3/2, 5/2 Fe(III)	(TPP)FeOClO ₃	CDCl ₃	26	¹ H	17	13 (210)	9.3	11.9	7.7
HS Fe(III) radical	(TPP)FeCl ⁺	CD ₂ Cl ₂	26	¹ H	32, 33	66.1 (170)	{37.6 34.4	-12.4	29.5
LS Fe(III)	(TPP)Fe(Im) ₂ ⁺	CDCl ₃	29	¹ H	34	-16.6 (40)	4.9	6.2	6.3
HS, LS Fe(II)	(TPP)Fe(Me ₂ SO) _{<i>x</i>}	Me ₂ SO- <i>d</i> ₆	26	¹ H	14	12.2 (25)		phenyls 8.1, 7.8	
HS Fe(II)	(TPP)Fe(2-CH ₃ Im)	toluene- <i>d</i> ₈	25	¹ H	35	52.2 (18)	9.5	8.8	8.7
HS Fe(II)	(TPP)Fe(SBu) ⁻	Me ₂ SO- <i>d</i> ₆	26	¹ H	14	61.0 (30)	{10.9 8.2	{8.9 7.9	7.9
<i>S</i> = 1 Fe(II)	(TPP)Fe	C ₆ D ₆	25	¹ H	9a	4.7 (15)	20.8	12.5	12.5
LS Fe(II)	(TPP)Fe(CO)	toluene- <i>d</i> ₈	27	¹ H	36	8.9 (~1)	7.5	8.1	7.5
HS Mn(III)	(TPP)MnO ₂ ⁻	Me ₂ SO	25	² H	<i>b</i>	32 (80)		phenyls 7.8	
	(TPP)MnCl	CDCl ₃	35	¹ H	16	-21.5 (~650)	~7	8.1	7.3
	(TPP)Mn(Me ₂ SO) _{<i>x</i>} ⁺	Me ₂ SO	25	² H	<i>b</i>	-26 (120)		phenyls 7.9	
HS Mn(II)	(TPP)Mn(Me ₂ SO) _{<i>x</i>}	Me ₂ SO	25	² H	<i>b</i>	34.3 (160)		phenyls 8.2	

^a Signals are referenced to (CH₃)₄Si, and downfield shifts are given positive sign. Abbreviations: HS, high spin; LS, low spin. ^b This work.

first-order magnetic behavior over the temperature range -30 to +30 °C. Similar spectra were obtained at 28 °C in Me₂SO solvent, except the deuterium pyrrole signal was appreciably broader (see Table I).

Visible spectra recorded after NMR examination retained the predominant 437-, 565-, and 609-nm bands of (TPP)FeO₂⁻,⁵ although in the presence of excess KO₂ appearance of a broad Soret absorption and bands at 583 and 635 nm was evident within 3 h of sample preparation or with heating of the solution. Appearance of these decomposition product bands was coincident with observation of a pyrrole deuterium NMR signal at 6.4 ppm. This minor 6.4-ppm signal could actually be detected within minutes of sample preparation. In the absence of excess KO₂, the predominant porphyrin decomposition product was the iron(III) μ -oxo dimer species, as judged by appearance of a pyrrole deuterium signal at 13.7 ppm.^{9b}

A solution magnetic moment of $\geq 5.6 \mu_B$ was obtained by the Evans¹¹ method for (TPP)FeO₂⁻ generated through addition of 2.0 equiv of KO₂-crown ether complex to (TPP)FeCl (Me₂SO solvent, 25 °C, Me₄Si reference). A lower limit is placed on the value due to apparent partial decomposition of the complex during the few minutes between sample preparation and transfer to the NMR spectrometer.

Examination of the (OEP)Fe reaction product was complicated due to its high reactivity, and (OEP)FeO₂⁻ was studied in only a cursory manner. A broad proton NMR signal at 32 ppm (Me₂SO-*d*₆ solvent, 28 °C, Me₄Si reference) for the methylene protons was rapidly replaced by signals near 15 ppm. The decomposition product has not been identified, but it is not the iron(III) μ -oxo dimer. Corresponding changes were observed in the visible spectrum, with appearance of a shoulder at 395 nm associated with decomposition of the complex.

Manganese Porphyrins. Parallel NMR measurements were conducted for the (TPP)MnO₂⁻ complex, which has been described as either a peroxomanganese(III) or a superoxomanganese(II) species.³ Deuterium NMR spectra are shown in Figure 3 for Me₂SO solutions of various manganese porphyrin species, and specific resonance values are listed in Table I. The parent (TPP)MnCl in Me₂SO solution (Figure 3a) exhibits an upfield pyrrole deuterium resonance (-26 ppm) much as observed previously for proton NMR spectra in chloroform solution.¹⁶ Addition of 2 equiv

or more of KO₂, either as the solid or as the crown ether complex, serves to generate a new species earlier identified as (TPP)MnO₂⁻.³ Visible-UV spectra of solutions prepared for NMR measurements match those previously reported for this adduct.³ Deuterium NMR spectra of this species (Figure 3b,c) are reminiscent of those for the manganese(II) species dissolved in Me₂SO (Figure 3d,e). A solution magnetic moment of 5.0 μ_B (Evans method, Me₂SO solvent, 25 °C, Me₄ reference) was observed for the (TPP)MnO₂⁻ complex. It should be noted that the (TPP)MnO₂⁻ complex is qualitatively more stable than the iron derivative and that decomposition yields predominantly the manganese(III) (Me₂SO or chloro) complex, rather than a modified porphyrin or μ -oxo dimer.

Discussion

Correlations between metalloporphyrin electronic structure and proton NMR contact shift values are now well-defined for the first-row transition series.^{9,17} Thus, a large downfield contact shift for the pyrrole proton signals of a TPP complex is associated with unpaired spin in the σ -type $d_{x^2-y^2}$ orbital. On the other hand, depopulation of $d_{x^2-y^2}$ and single population of π -type d_{xz} and/or d_{yz} orbitals has been consistently associated with an upfield pyrrole proton contact shift.¹⁸ On the basis of these accepted correlations, the downfield pyrrole deuterium signals for both (TPP)FeO₂⁻ and (TPP)MnO₂⁻ imply single population of the $d_{x^2-y^2}$ orbital. This clearly dictates a superoxomanganese(II) formulation, as the d^4 manganese(III) porphyrin has $d_{x^2-y^2}$ depopulated. Empirical comparison of spectra in Figure 3 is also most convincing in terms of oxidation-state assignment.

Both high-spin iron(II) and iron(III) porphyrins have $d_{x^2-y^2}$ singly occupied, and as a consequence, pyrrole proton signals are observed in a downfield region between 50 and 80 ppm. Pyrrole proton line widths (Table I) are generally 1 order of magnitude larger for iron(III) vs. iron(II) porphyrins and serve to distinguish

(16) La Mar, G. N.; Walker, F. A. *J. Am. Chem. Soc.* **1975**, *97*, 5103-5107.

(17) (a) Shimomura, E.; Goff, H. *J. Am. Chem. Soc.* **1980**, *102*, 31-37. (b) Boersma, A. D.; Goff, H. M. *Inorg. Chem.* **1982**, *21*, 581-586.

(18) Although comparisons can only properly be made from contact shift values, the dipolar shift values for species examined here must be negligible, as judged by the very small shifts for porphyrin phenyl resonances.

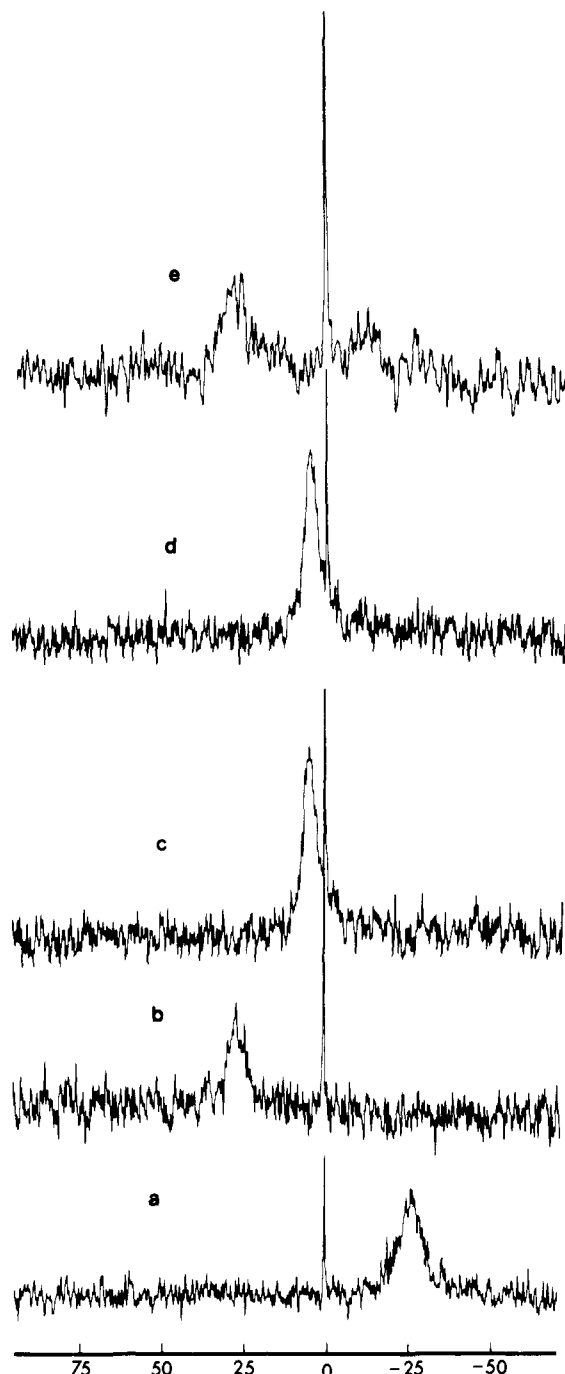


Figure 3. Deuterium NMR spectra of selectively deuterium-labeled manganese porphyrin species, with 4 mM manganese porphyrin and Me_2SO solvent at 25 °C: (a) (TPP-pyrrole- d_8)MnCl; (b) (TPP-pyrrole- d_8)MnO $_2^-$; (c) TPP-phenyl- d_{20} MnO $_2^-$; (d) (TPP-phenyl- d_{20})Mn; (e) (TPP-pyrrole- d_8)Mn. The ppm scale is referenced to Me_4Si , and downfield shifts are given positive signs. The sharp signal is due to natural-abundance deuterium in Me_2SO solvent.

these two oxidation states. Other identified spin- and oxidation-state species are described in Table I. Formulation of (TPP)FeO $_2^-$ as a low-spin iron(III), intermediate-spin ($S = 3/2$) iron(III), or intermediate-spin ($S = 1$) iron(II) porphyrin complex must be ruled out as these species have upfield pyrrole proton NMR signals. An iron(IV) oxidation state is expected to yield an upfield pyrrole deuterium signal associated with depopulation of $d_{x^2-y^2}$. A low-spin iron(I) configuration would be isoelectronic with cobalt(II) porphyrins, for which only small downfield dipolar shifts are observed.^{9b} Thus, on the basis of the observed shift pattern and a relatively broad pyrrole deuterium (proton) NMR signal, the (TPP)FeO $_2^-$ species is best formulated as a peroxyiron(III) adduct.

Solution magnetic moments are further supportive of the oxidation-state assignments made by NMR correlations. A magnetic moment approaching the spin-only value of $5.9 \mu_B$ expected for high-spin iron(III) is consistent with the peroxyiron(III) configuration. The alternate high-spin superoxyiron(II) resonance form would likely exhibit strong antiferromagnetic coupling between the $S = 2$ iron center and the $S = 1/2$ superoxide ion. Although the resulting $S = 3/2$ species would be ESR active ($S = 3/2$ iron(III) porphyrins yield $g = 4$ signals),¹⁹ the $\geq 5.6\text{-}\mu_B$ magnetic moment value is quite elevated for an $S = 3/2$ configuration. In the absence of strong antiferromagnetic coupling the total "spin-only" moment for a $S = 2 + S = 1/2$ species would be $5.20 \mu_B$ —significantly below the measured $\geq 5.60\text{-}\mu_B$ value. A solution magnetic moment of $5.0 \mu_B$ was observed for (TPP)MnO $_2^-$. Although this value would be consistent with the d^4 configuration of manganese(III), the more reasonable assignment is that of a manganese(II) center with strong antiferromagnetic coupling to the unpaired spin on a superoxo ligand. This species seemingly provides a model for the spin-coupled low-spin iron(III) superoxo configuration of oxyhemoglobin.

Deuterium NMR results presented here merit further comment about molecular and electronic structures of superoxide reaction products. On the basis of variable-temperature NMR spectra and the magnetic moment, a monomeric structure is anticipated for (TPP)FeO $_2^-$. Thus, NMR spectra are quite sensitive to metal-metal antiferromagnetic coupling in known $\mu\text{-oxo}$ ^{9b} and $\mu\text{-peroxo}$ ²⁰ dimeric iron(III) porphyrins. Entries in Table I for these two dimeric species certainly do not approach those for (TPP)FeO $_2^-$. Reasonable Curie law behavior and absence of significant attenuation in the pyrrole deuterium resonance of (TPP)FeO $_2^-$ indicate that any oxygen bridging unit would have to be unique in providing only weak antiferromagnetic coupling. Less is unfortunately known about bridged manganese porphyrin species, but the results presented here provide no evidence for a dimeric structure.

Nuclear magnetic resonance spectroscopy is of particular value in demonstrating that the fourfold symmetry of the porphyrin ring is preserved in the (TPP)FeO $_2^-$ complex. Thus, if oxygen attack occurred at a pyrrole nitrogen atom, as has recently been demonstrated for carbene ligands,²¹ splitting of the pyrrole deuterium resonance would be anticipated. Oxygen attack at a meso carbon or pyrrole carbon position might likewise induce splitting of the downfield pyrrole signals of (TPP)FeO $_2^-$ and (TPP)MnO $_2^-$.

The (TPP)FeO $_2^-$ species is likely coordinated in both axial positions in Me_2SO solution. This suggestion is based on the upfield bias for pyrrole proton resonances of known bisligated complexes of high-spin iron(III) porphyrins.²² Thus, the signals for (TPP)Fe(Me_2SO) $_2^+$ of 66.8 ppm and for TPP(SO $_3$) $_4$ Fe(H_2O) $_2^{3-23}$ of 51 ppm are to be compared with the value of 60 ppm for (TPP)FeO $_2^-$ vs. the value of 79 ppm for five-coordinate complexes such as (TPP)FeCl (all at 25 °C). Bidentate coordination of O $_2^{2-}$ alone is not expected to yield a pyrrole proton signal at 60 ppm, on the basis of comparison of known bidentate coordination of nitrate ion and presumed bidentate coordination of sulfate ion, for which signals are observed at 73 ppm.²⁴ Unfortunately, lines are too broad to detect possible splitting of 3,5-phenyl deuterium signals that might indicate placement of the iron atom out of the porphyrin plane toward a single axial peroxy ligand.

(19) Reed, C. A.; Mashiko, T.; Bentley, S. P.; Kastner, M. E.; Scheidt, W. R.; Spartalian, K.; Lang, G. *J. Am. Chem. Soc.* **1979**, *101*, 2948–2958.

(20) (a) Chin, D.-H.; Del Gaudio, J.; La Mar, G. N.; Balch, A. L. *J. Am. Chem. Soc.* **1977**, *99*, 5486–5488. (b) Chin, D.-H.; La Mar, G. N.; Balch, A. L. *Ibid.* **1980**, *102*, 4344–4350.

(21) Latos-Grazynski, L.; Cheng, R.-J.; La Mar, G. N.; Balch, A. L. *J. Am. Chem. Soc.* **1981**, *103*, 4270–4272.

(22) (a) Zobrist, M.; La Mar, G. N. *J. Am. Chem. Soc.* **1978**, *100*, 1944–1946. (b) Mashiko, T.; Kastner, M. E.; Spartalian, K.; Scheidt, W. R.; Reed, C. A. *Ibid.* **1978**, *100*, 6354–6362.

(23) Goff, H. M.; Morgan, L. O. *Bioinorg. Chem.* **1978**, *9*, 61–79.

(24) (a) Phillippi, M. A.; Goff, H. M. *J. Chem. Soc., Chem. Commun.* **1980**, 455–456. (b) Phillippi, M. A.; Baenziger, N.; Goff, H. M. *Inorg. Chem.* **1981**, *20*, 3904–3911.

A small value for the zero-field-splitting parameter, D , is seemingly associated with the very broad NMR resonances observed for the $(\text{TPP})\text{FeO}_2^-$ complex. Proton^{9b,25} and carbon-13^{26,27} NMR studies have served to demonstrate modulation of line widths through zero-field splitting of the otherwise isotropic d^5 ion. Axial coordination by two ligands makes the iron porphyrin pseudooctahedral, and thus the ligand field is more nearly isotropic. In this regard, coordination by peroxo and solvent ligands is expected to induce the small zero-field splitting associated with severe NMR line broadening. The essentially linear Curie law plot is also supportive of small zero-field splitting, as the quadratic temperature dependence for induced dipolar shifts leads to curvature of the Curie plot for other weak-field anionic ligands.^{25,28} A value considerably less than the $D = 5.9 \text{ cm}^{-1}$ measured for $(\text{TPP})\text{FeCl}_2^{29}$ is expected for $(\text{TPP})\text{FeO}_2^-$. Although D is diminished in $(\text{TPP})\text{FeO}_2^-$ due to an increased axial ligand field, a sizeable rhombic perturbation (as represented by the zero-field-splitting parameter E) may be invoked to explain the ESR $g = 2, 4.2, \text{ and } 8$ values.⁵ A ratio of $E/D \approx 0.1$ is necessary to produce a rhombic $g = 4$ signal, and the lower D value thus effectively contributes to the rhombicity. Differing pyrrole deuterium linewidths for Me_2SO and acetonitrile solvents may be explained by presence or absence of a coordinated solvent ligand or by specific solvation of the peroxo ligand.

(25) (a) La Mar, G. N.; Eaton, G. R.; Holm, R. H.; Walker, F. A. *J. Am. Chem. Soc.* **1973**, *95*, 63-75. (b) Walker, F. A.; La Mar, G. N. *Ann. N.Y. Acad. Sci.* **1973**, *206*, 328-348.

(26) Mispelter, J.; Momenteau, M.; Lhoste, J.-M. *J. Chem. Soc., Dalton Trans.* **1981**, 1729-1734.

(27) Goff, H. M.; Shimomura, E. T.; Phillippi, M. A. *Inorg. Chem.*, in press.

(28) Behere, D. V.; Birdy, R.; Mitra, S. *Inorg. Chem.* **1982**, *21*, 386-390.

(29) (a) Behere, D. V.; Marathe, V. R.; Mitra, S. *J. Am. Chem. Soc.* **1977**, *99*, 4149-4150. (b) Behere, D. V.; Birdy, R.; Mitra, S. *Inorg. Chem.* **1981**, *20*, 2786-2789.

In conclusion, one must ask why the superoxide anion serves as an oxidizing agent for the iron(II) porphyrin but seemingly does not oxidize the manganese(II) analogue. A clear explanation is not found in available redox potential differences. For example, the $\text{M(III)} \rightarrow \text{M(II)}$ potentials for chloro complexes of Fe(III) and Mn(III) tetraphenylporphyrins in methylene chloride solvent are -0.29^{30} and -0.33 V^{31} (vs. SCE), respectively. Potentials are dependent on the nature of the anionic ligand, however, and it would be of interest to measure values for the peroxo and superoxo complexes. The role of solvent coordination at the second axial site may well be important in controlling electron transfer to a coordinated superoxo ligand. In this regard, it should be noted that both manganese(II) and manganese(III) porphyrins show a preference for five-coordination,³¹ whereas the iron derivatives will certainly bind appropriate solvent ligands.²²

Acknowledgment. Support from NIH grant GM 28831-02 and NSF grant CHE 79-10305 is gratefully acknowledged. We wish to thank Mr. Arden Boersma and Mr. Scott Wright for preparation of selected deuterated porphyrins.

Registry No. $(\text{TPP})\text{FeO}_2^-$, 83160-26-3; $(\text{TPP})\text{FeCl}_2$, 16456-81-8; $(\text{TPP})\text{Fe}(\text{Me}_2\text{SO})_2^+$, 68179-07-7; $(\text{TPP})\text{MnO}_2^-$, 83160-27-4; $(\text{TPP})\text{Mn}(\text{Me}_2\text{SO})^+$, 83160-28-5; $(\text{TPP})\text{Mn}(\text{Me}_2\text{SO})$, 83160-29-6; $(\text{TPP})\text{MnCl}_2$, 32195-55-4; KO_2 , 12030-88-5; D_2 , 7782-39-0.

(30) Bottomley, L. A.; Kadish, K. M. *Inorg. Chem.* **1981**, *20*, 1348-1357.

(31) Kadish, K. M.; Kelly, S. *Inorg. Chem.* **1979**, *18*, 2968-2971.

(32) Phillippi, M. A.; Shimomura, E. T.; Goff, H. M. *Inorg. Chem.* **1981**, *20*, 1322-1325.

(33) Gans, P.; Marchon, J.-C.; Reed, C. A.; Regnard, J.-R. *Nouv. J. Chim.* **1981**, *5*, 203-204.

(34) La Mar, G. N.; Walker, F. A. *J. Am. Chem. Soc.* **1973**, *95*, 1782-1790.

(35) Goff, H. M.; La Mar, G. N. *J. Am. Chem. Soc.* **1977**, *99*, 6599-6606.

(36) Wayland, B. B.; Mehne, L. F.; Swartz, J. J. *J. Am. Chem. Soc.* **1978**, *100*, 2379-2383.

α -Hydride Elimination from Methylene and Neopentylidene Ligands. Preparation and Protonation of Tungsten(IV) Methylidyne and Neopentylidyne Complexes¹

S. J. Holmes, D. N. Clark, H. W. Turner, and R. R. Schrock*

Contribution from the Department of Chemistry, Massachusetts Institute of Technology, Cambridge, Massachusetts 02139. Received December 22, 1981

Abstract: $\text{W}(\text{CCMe}_3)(\text{CHCMe}_3)(\text{CH}_2\text{CMe}_3)(\text{dmpe})$ ($\text{dmpe} = \text{Me}_2\text{PCH}_2\text{CH}_2\text{PMe}_2$) reacts with dmpe to give 2,2,5,5-tetramethyl-*trans*-3-hexene and $\text{W}(\text{CCMe}_3)(\text{dmpe})_2(\text{H})$. Addition of HCl to $\text{W}(\text{CCMe}_3)(\text{dmpe})_2(\text{H})$ yields $\text{W}(\text{CCMe}_3)(\text{dmpe})_2\text{Cl}$. $\text{W}(\text{CCMe}_3)(\text{PMe}_3)_4\text{Cl}$ can be prepared by reducing $\text{W}(\text{CCMe}_3)(\text{PMe}_3)_3\text{Cl}_3$ in the presence of PMe_3 . The reaction between $\text{WCl}_2(\text{PMe}_3)_4$ and AlMe_3 gives $\text{W}(\text{CH})(\text{PMe}_3)_4\text{Cl}$, which, when treated with dmpe , yields $\text{W}(\text{CH})(\text{dmpe})_2\text{Cl}$. Protonation of $\text{W}(\text{CR})(\text{dmpe})_2\text{Cl}$ ($\text{R} = \text{H}$ or CMe_3) yields cationic, pentagonal bipyramidal methylidyne hydride and neopentylidyne hydride complexes, $[\text{W}(\text{CR})(\text{H})(\text{dmpe})_2\text{Cl}]^+$. In the case where $\text{R} = \text{H}$, the hydride and methylidyne protons exchange intramolecularly at 25 °C on the NMR time scale. Protonation of $\text{W}(\text{CR})(\text{PMe}_3)_4\text{Cl}$ with $\text{CF}_3\text{SO}_3\text{H}$ yields grossly distorted methylene and neopentylidene complexes because (it is believed) four PMe_3 ligands cannot, for steric reasons, form a pentagonal-bipyramidal molecule with four PMe_3 ligands and a hydride in the pentagonal plane. Protonation of $\text{W}(\text{CH})(\text{PMe}_3)_4\text{Cl}$ with HCl yields pentagonal-bipyramidal $\text{W}(\text{CH})(\text{H})(\text{PMe}_3)_3\text{Cl}_2$. An analogous complex, $\text{W}(\text{CH})(\text{H})(\text{PMe}_3)_3(\text{Cl})(\text{BH}_3\text{CN})$, can be prepared by reacting $[\text{W}(\text{CH}_2)(\text{PMe}_3)_4\text{Cl}]^+\text{CF}_3\text{SO}_3^-$ with NaBH_3CN . These results suggest that under the right circumstances " α -hydride elimination" from an alkylidene ligand to give an alkylidyne ligand is facile and reversible but that sometimes formation of a distorted alkylidene (including methylene) is as far as the α -elimination reaction can proceed. The driving force for α elimination can be viewed as an oxidation of "tungsten(IV)" to "tungsten(VI)".

The first isolated "tungsten(VI)" alkylidene complex was $\text{W}(\text{CCMe}_3)(\text{CHCMe}_3)(\text{CH}_2\text{CMe}_3)\text{L}_2$ ($\text{L} = \text{PMe}_3$ or 0.5dmpe).² Now oxo alkylidene complexes^{3a} such as $\text{W}(\text{O})(\text{CHR})(\text{PMe}_3)_2\text{Cl}_2$

($\text{R} = \text{H}, \text{Pr}, \text{Ph}, \text{CMe}_3$) and analogous imido alkylidene complexes^{3b} have been prepared and characterized. In each type of complex the distortion of the alkylidene ligand (which is characterized by a small $\text{M}=\text{C}-\text{H}$ angle and a low value for J_{CH_2})⁴

(1) Multiple Metal-Carbon Bonds. 26. For part 25, see ref 23.

(2) Clark, D. N.; Schrock, R. R. *J. Am. Chem. Soc.* **1978**, *100*, 6774.

(3) (a) Wengrovius, J. H.; Schrock, R. R. *Organometallics* **1982**, *1*, 148.

(b) Pedersen, S.; Schrock, R. R., in press.